Title

Nur77 Is Upregulated in B-1a Cells by Chronic Self-Antigen Stimulation and Limits Generation of Natural IgM Plasma Cells

Journal

ImmunoHorizons, 1(9)

ISSN

2573-7732

Authors

Huizar, John
Tan, Corey
Noviski, Mark
et al.

Publication Date

2017-11-01

DOI

10.4049/immunohorizons.1700048

Peer reviewed

HHS Public Access

Author manuscript

Immunohorizons. Author manuscript; available in PMC 2017 November 15.

Published in final edited form as:

Immunohorizons. 2017 November 1; 1(9): 188–197. doi:10.4049/immunohorizons.1700048.

Nur77 Is Upregulated in B-1a Cells by Chronic Self-Antigen Stimulation and Limits Generation of Natural IgM Plasma Cells

John Huizar[*], **Corey Tan**[†], **Mark Noviski**[†], **James L. Mueller**[‡], and **Julie Zikherman**[‡]

[*]Howard Hughes Medical Institute Medical Fellows Program, University of California, San Francisco, San Francisco, CA 94143

[†]Biomedical Sciences Graduate Program, University of California, San Francisco, San Francisco, CA 94143

[‡]Rosalind Russell and Ephraim P. Engleman Arthritis Research Center, Division of Rheumatology, Department of Medicine, University of California, San Francisco, San Francisco, CA 94143

Abstract

B-1a cells are a unique population of innate-like B cells with a highly restricted and self-reactive BCR repertoire. Preimmune “natural” IgM produced by B-1a–derived plasma cells is essential for homeostatic clearance of cellular debris and forms a primary layer of protection against infection. In this study, we take advantage of a fluorescent reporter of BCR signaling to show that expression of the orphan nuclear hormone receptor Nur77 is upregulated under steady-state conditions in self-reactive B-1a cells in response to chronic Ag stimulation. Nur77-deficient mice exhibit elevated natural serum IgM (but not IgG) and marked expansion of IgM plasma cells of B-1a origin. Moreover, we show that Nur77 restrains the turnover of B-1a cells and the accumulation of immature IgM plasma cells. Thus, we identify a new critical negative-regulatory pathway that serves to maintain B-1a cells in a quiescent state in the face of chronic endogenous Ag stimulation.

INTRODUCTION

B-1a cells are a unique subset of innate-like B cells that survey body cavities and form a first line of defense against pathogens (1). Unlike bone marrow (BM)-derived B-2 cells, B-1a cells are generated almost exclusively during fetal development and are maintained via self-renewal in the periphery (1). The B-1a BCR repertoire is highly restricted and selected on the basis of germline-encoded reactivity to self-antigens, such as phosphatidylcholine (PtC), which is exposed on the membranes of dying cells (1–3). It is thought that a significant proportion of so-called preimmune “natural” serum IgM is derived from the B-1a

Address correspondence and reprint requests to: Dr. Julie Zikherman, University of California, San Francisco Medical Center, 513 Parnassus Avenue, Room HSW1201E, Box 0795, San Francisco, CA 94143-0795. julie.zikherman@ucsf.edu.

ORCIDs: 0000-0002-5696-6766 (C.T.); 0000-0001-8072-1059 (M.N.); 0000-0002-0873-192X (J.Z.).

The online version of this article contains supplemental material.

DISCLOSURES

The authors have no financial conflicts of interest.

compartment in the steady-state (1). Natural serum IgM, like precursor B-1a cells, harbors autoreactivity, as well as cross-reactivity to bacterial polysaccharides, and it plays an important role in modulating the early immune response to infection and maintaining tissue homeostasis by opsonizing cell debris and oxidized low-density lipoprotein cholesterol for clearance (3). B-1a–derived IgM Ab-secreting cells (ASCs) with heterogeneous phenotypes have been identified in the BM and spleen (4). B-1a cells are maintained in a quiescent state in the face of chronic self-antigen stimulation, in part by constitutive expression of inhibitory coreceptors that suppress BCR signaling (5–8). However, the factors that regulate IgM ASC generation under steady-state conditions have not been fully elucidated.

Nr4a1–3 encode a small family of orphan nuclear receptors (Nur77, Nurr1, and Nor1, respectively) that share significant structural similarities in their DNA-binding and ligand-binding domains (9). These proteins are rapidly induced in response to BCR and TCR stimulation, as well as other mitogenic stimuli, and they are thought to be constitutively active, with no known endogenous ligands. *Nr4a* genes play critical roles in immune cells, mediating Ag-induced apoptosis in T cell hybridomas, and deletion of self-reactive thymocytes (10–12). However, *Nr4a1*$^{-/-}$ mice are healthy and have no overt defect in negative selection, likely as a result of *Nr4a* gene redundancy (13). In contrast, germline deletion of both *Nr4a1* and *Nr4a3* in mice leads to rapid development of acute myeloid leukemia, which is mediated, in part, by derepression of *c-Myc* (14, 15). Similarly, conditional deletion of all three *Nr4a* genes in thymocytes results in dysregulation of *Foxp3* and complete loss of all regulatory T cells (16, 17). However, *Nr4a1* does have nonredundant functions; *Nr4a1* is essential for development of the “patrolling” Ly6C^{low} monocyte subset (18–20), and it suppresses LPS-induced inflammatory responses in Ly6C^{hi} “inflammatory” monocytes (21). However, despite their rapid upregulation in response to BCR signaling, the function of the *Nr4a* genes in normal B cell biology is unknown.

We have recently characterized a reporter of *Nr4a1* gene expression, Nur77-eGFP transgenic (Tg), whose expression scales with the intensity of BCR stimulation in vitro and is upregulated in Ag-specific B cells in vivo in immunized mice (22, 23). We have shown that endogenous Ag is necessary and sufficient for Nur77-eGFP expression in follicular B-2 cells in vivo (23).

In this article, we show that Nur77-eGFP reporter expression is highly upregulated in B-1a cells, particularly in those with self-reactive PtC-binding BCRs. We find that Nur77-deficient (*Nr4a1*$^{-/-}$) mice have an elevated level of natural serum IgM (but not IgG) under steady-state conditions. We show that increased serum IgM in these mice is B-1a derived, and loss of Nur77 in B-1a cells is sufficient to produce this phenotype. In the absence of Nur77, we observe marked expansion of mature IgM plasma cells (PCs), as well as disproportionate accumulation of immature IgM PCs. B-1a cells turnover more quickly but do not accumulate in the absence of Nur77. These observations support a model in which chronic stimulation of self-reactive B-1a cells by endogenous Ags upregulates Nur77 expression; this, in turn, restrains the differentiation of B-1a cells into natural IgM PCs. Thus, we identify a critical negative-regulatory pathway that maintains B-1a cells in a quiescent state in the face of chronic Ag stimulation.

MATERIALS AND METHODS

Mice

Nur77-eGFP mice and hen egg lysozyme–specific BCR (IgHEL) Tg mice (MD4 line) were described previously (23, 24). BoyJ and *Nr4a1*$^{-/-}$ mice were from The Jackson Laboratory (13). All mice were housed in a specific pathogen–free facility at University of California, San Francisco, according to university and National Institutes of Health guidelines.

Abs and reagents

Reagents used in this study include streptavidin (SA) and Abs to B220, CD4, CD5, CD19, CD21, CD23, CD43, CD44, CD93 (AA4.1), CD45.1, CD45.2, CD138, Irf4, IgM, IgM(a), IgM(b), IgD, IgD(a), IgD(b) conjugated to biotin or fluorophores (BioLegend, eBio-science, BD, or Tonbo); p-Erk Ab (clone 194G2; Cell Signaling Technology); goat anti-mouse Igκ (SouthernBiotech); ELISA and ELISPOT reagents: 96-well plates for ELISA (Costar) and mixed cellulose ester MultiScreen filter plates for ELISPOT (Miltenyi Biotec), SA-HRP, SA–alkaline phosphatase, anti-mouse IgM, IgH+L, IgG1, 2c, 3, IgA unlabeled or conjugated to biotin or HRP (SouthernBiotech), NP-29–BSA, PC-2–BSA (Biosearch Technologies), TMB (Sigma), BCIP/NBT Substrate (Vector Laboratories); 100 nm rhodamine PtC liposomes (FormuMax Scientific); NP-61–Ficoll (Biosearch Technologies); and ibrutinib (J. Taunton, University of California, San Francisco). Ibrutinib was used at 50 nM working concentration for in vitro B cell culture. PtC liposomes were used at a dilution of 1:1000 (50 mM) for staining and in vitro stimulation. Complete culture media was prepared with RPMI 1640 + L-Glutamine (Corning-Life Technologies), Penicillin Streptomycin L-Glutamine, HEPES buffer (10 mM), 2-ME (55 mM), sodium pyruvate, Non-Essential Amino Acids Solution (all from Life Technologies), and 10% heat-inactivated FBS (Omega Scientific).

Flow cytometry and data analysis

Cells were collected on a BD Fortessa and analyzed with FlowJo software (v 9.9.5; TreeStar). Statistical analysis and graphs were generated using Prism 6 (GraphPad). Scanned images of ELISPOTs were counted using ImageJ software (National Institutes of Health).

Intracellular PC staining

Cells were permeabilized and stained, according to the manufacturer's protocol, to detect intracellular IgM (BD Cytofix/Cytoperm kit).

Intracellular phosphoflow staining

Peritoneal cavity (PerC) cells were stimulated for 5 min with various doses of anti-κ Ab, fixed, permeabilized with MeOH, and stained to detect p-Erk, as previously described (23).

BM chimeras

Host mice were irradiated twice with 330 mCi, 4 h apart, and injected i.v. with 10^6 donor A BM cells mixed with 10^6 donor B BM cells or with 6.75×10^5 donor A BM cells and 6.75×10^5 donor B PerC cells.

ELISA and ELISPOT

ELISA and ELISPOT were performed as previously described (25). For detection of total serum IgM and IgG, serum Ig was captured using goat anti-mouse IgM or IgG(H+L) (1 μg/ml) and detected using polyclonal HRP-conjugated Abs to IgM, IgG1, IgG2a, IgG2b, or IgG3 (SouthernBiotech) at a dilution of 1:3000. For PC ELISA, plates were coated with PC-2–BSA or BSA alone (5 μg/ml), and sera were added at 1:5 starting dilution and serially diluted 2-fold. Titers were calculated by subtracting the BSA signal from the PC BSA signal. NP-binding IgM was captured using plates coated with NP-29–BSA (1 μg/ml) in PBS. For ELISPOT, wells were coated with goat anti-mouse IgM (10 μg/ml). BM and spleen cells were plated in duplicate at 5×10^5 cells per well and 2.5×10^5 cells per well, respectively, and serially diluted 2-fold. Spots were detected with goat anti-mouse IgM-biotin (1:10,000), followed by SA–alkaline phosphatase (1:1,000), and developed with BCIP/NBT Substrate.

BrdU labeling and staining

Mice weretreated with 0.8 μg/ml BrdU in drinking water for 2 wk. Cells were stained as per the manufacturer's protocol (BrdU Flow Kit; BD).

Immunization

One-hundred micrograms of NP-61–Ficoll in PBS was injected i.p., and serum was collected at baseline and weekly for 3 wk.

RESULTS

Nur77-eGFP reporter expression is upregulated in B-1a cells in an Ag-dependent manner

B-1a cells are thought to be selected by reactivity to self-antigen(3). To determine the intensity of endogenous Ag stimulation of B-1a cells at steady-state, we took advantage of the Nur77-eGFP reporter. PerC B-1a cells ($CD5^+$ $CD43^+$ $CD23^-$ $CD19^+$) have much higher steady-state expression of Nur77-eGFP than do PerC B-2 cells, suggesting that this population is subject to chronic or intermittent antigenic stimulation in vivo under steady-state conditions (Fig. 1A–C) (1).

To confirm that Nur77-eGFP in PerC B cells reflects Ag-dependent signaling, we sought to eliminate Ag in vivo. To do so, we introduced the IgHEL Tg onto the Nur77-eGFP reporter background without coexpression of cognate HEL Ag (24). Very few B-1a cells develop in IgHEL Tg mice in the absence of cognate Ag (Fig. 1D). Although the majority of B-2 cells in the PerC express the HEL-specific BCR (identified by the IgM^a allotype), the few B-1a cells that arise almost exclusively express endogenous IgM^b BCRs, suggesting that only "escapee" B cells capable of recognizing endogenous Ag are selected into this compartment (Fig. 1E, Supplemental Fig. 1A). IgM^b escapees in all peritoneal B cell compartments express high levels of GFP comparable to reporter mice with an unrestricted BCR repertoire (Fig. 1F). In contrast, IgM^a HEL-specific B-2 and B-1b B cells lose GFP expression in the absence of endogenous cognate Ag (Fig. 1F, Supplemental Fig. 1B). Because B-1a cell development is dependent upon endogenous Ag recognition, this comparison was not possible for B-1a cells. Our data suggest that endogenous Ag-dependent signaling is

required for the development of B-1a cells and drives high levels of Nur77-eGFP reporter expression in B-1a cells at steady-state, consistent with the well-described self-reactivity of this compartment (3).

Nur77-eGFP expression identifies self-reactive PtC-specific B-1a B cells in vivo

Recent deep sequencing of the B-1a H chain repertoire by Herzenberg and colleagues (2) reveals that four PtC-binding CDR3 sequences account for more than one third of all of the CDR3s identified in peritoneal B-1a cells. Moreover, this specificity is restricted to the $CD5^+$ B-1a B cell compartment in the PerC (26). The exact nature of PtC-containing Ags in vivo is not known, but they may include dying cells and senescent erythrocytes (3). Staining of PerC cells with rhodamine-conjugated PtC liposomes confirmed marked enrichment of PtC-binding BCR specificities among B-1a, but not B-1b or B-2, cells (Fig. 2A, Supplemental Fig. 1C) (26). Interestingly, PtC-binding B1-a cells express significantly higher Nur77-eGFP than do PtC-negative B-1a B cells stained directly ex vivo (Fig. 2B, 2C). PtC liposomes induce Nur77-eGFP upregulation in vitro in a Btk-dependent manner and do so only in PtC-binding B-1a cells (Fig. 2D). Similarly, even in the absence of exogenous stimulation, Nur77-eGFP increases in B-1a cells in vitro in a Btk-dependent manner, suggesting that this rise in GFP is BCR dependent and presumably driven by bound self-antigens (Fig. 2D). Not only is endogenous Ag required for Nur77-eGFP expression in PerC B cells in vivo, it is sufficient to upregulate Nur77-eGFP in B-1a cells.

Excess natural serum IgM in Nr4a1$^{-/-}$ mice arises from the B-1a compartment

We next sought to identify the function of Nur77 in B-1a cells by studying mice with germline deletion of *Nr4a1* (13). Immature and mature B cell subsets in the BM, spleen, PerC, and lymph nodes are grossly unaffected by loss of Nur77 (Supplemental Fig. 1D, 1E). However, total serum IgM is markedly increased in *Nr4a1*$^{-/-}$ mice relative to wild-type (WT) mice (Fig. 3A). With the exception of a modest reduction in serum IgG1 in *Nr4a1*$^{-/-}$mice, other IgG isotypes do not differ significantly among genotypes (Fig. 3B). Because of its origin in the B-1a compartment, natural IgM is enriched for canonical B-1a specificities. Indeed, we found that the excess serum IgM in *Nr4a1*$^{-/-}$ mice contains a typical proportion of canonical phosphorylcholine-binding IgM Ab (Supplemental Fig. 1F–H).

To confirm that B-1a cells are indeed the source of excess serum IgM in *Nr4a1*$^{-/-}$ mice, we generated chimeras with selective *Nr4a1* deficiency in B-1a cells. We took advantage of an established strategy that capitalizes on the predominant fetal origin of B-1a cells: we reconstituted irradiated WT recipients with IgH^a allotype–marked donor BM mixed with IgH^b allotype–marked peritoneal lavage fluid from WT or *Nr4a1*$^{-/-}$ donors (Fig. 3C) (1, 27). As expected, we observed the predominant contribution of IgH^b PerC cell progeny to the B-1a compartment of hosts (Supplemental Fig. 1I, 1J). Recipients receiving *Nr4a1*$^{-/-}$ PerC cells had markedly elevated serum IgM^b relative to those receiving *Nr4a1*$^{+/+}$ PerC cells (Fig. 3D). Conversely, IgM^a emanating from donor BM did not differ between recipients. To exclude a role for B-2 cells in contributing to this phenotype, we also generated conventional competitive BM chimeras consisting of a 50:50 mixture of donor IgH^a BM mixed with WT or *Nr4a1*$^{-/-}$ IgH^b allotype–marked BM. Because of their fetal origin, B-1a cells are poorly

reconstituted by adult BM, and most IgM in these mice originates from B-2 B cells. We see no significant difference in serum IgM^a or IgM^b among these recipients, irrespective of whether they received *Nr4a1*-sufficient or -deficient BM (Fig. 3E). Taken together, these data strongly argue that B-1a cells, rather than B-2 B cells, are responsible for the increase in serum IgM in *Nr4a1*$^{-/-}$ mice and that Nur77 acts in a B cell–intrinsic manner to restrain natural IgM production.

IgM ASCs are expanded in Nr4a1$^{-/-}$ mice

We next sought to identify the an atomic and cellular sources of excess serum IgM in *Nr4a1*$^{-/-}$ mice. We observed elevated levels of IgM secretion by cultured splenocytes and, more notably, by cultured BM cells from *Nr4a1*$^{-/-}$ mice (Supplemental Fig. 2A). To identify IgM-secreting cells, BM cells were stained for membrane IgM and then stained intracellularly for cytoplasmic IgM using a distinct fluorophore (27). We identified an expanded population of putative IgM ASCs in BM and spleen of *Nr4a1*$^{-/-}$ mice but no change in the number of isotype-switched PCs (i.e., cytoplasmic IgM^- $CD138^{hi}$ $B220^{lo}$ cells) (Fig. 4A, 4B, Supplemental Fig. 2B). These IgM ASCs retain many phenotypic features of Blimp1-dependent canonical PCs, including high Irf4 and CD138 expression (Supplemental Fig. 2C) (4, 27). Finally, we confirmed by ELISPOT that bona fide IgM ASCs are indeed expanded in *Nr4a1*$^{-/-}$ mice (Fig. 4C–E).

Nur77 deficiency perturbs selection of the natural IgM PC repertoire

We find that PtC specificities are enriched among IgM PCs from WT and *Nr4a1*$^{-/-}$ mice (Supplemental Fig. 2D). Further, the absolute number of PtC-specific IgM PCs is expanded in *Nr4a1*$^{-/-}$ mice, consistent with a B-1a cell origin for these cells (Supplemental Fig. 2E). Nevertheless, despite absolute expansion of PtC-binding IgM PCs, their relative frequency is decreased in *Nr4a1*$^{-/-}$ mice (Supplemental Fig. 2F), and this is disproportionate to a more modest reduction in PtC-specific B-1a cells in *Nr4a1*$^{-/-}$mice (Supplemental Fig. 2G–I). This suggests that Nur77 imposes selective pressures that shape the B-1a cell repertoire and the natural IgM PC repertoire.

Accumulation of phenotypically immature IgM PCs in *Nr4a1*$^{-/-}$ mice

As PC differentiation proceeds, high m.w. isoforms of CD45 (CD45R/B220) undergo regulated splicing and are gradually replaced with the low m.w. CD45 isoform, CD45RO (28). A disproportionately high fraction of IgM PCs in *Nr4a1*$^{-/-}$ mice retained high surface B220 expression, suggesting accumulation of newly formed PCs or plasmablasts (PBs) (Fig. 5A–E, Supplemental Fig. 2C). Although IgM PCs, in contrast to isotype-switched PCs, retain surface IgM expression (Fig. 4A), we found little to no GFP expression in mature $B220^{lo}$ IgM PCs (Fig. 5F) (29). This is in marked contrast to elevated Nur77-eGFP expression in B-1a precursors (Fig. 5F). Importantly, $B220^{hi}$ IgM ASCs express an intermediate amount of Nur77-eGFP, suggesting that these cells are recently generated PCs, given a GFP half-life ~ 24 h (Fig. 5F). This expression pattern suggested to us that Nur77 may be active predominantly in the precursor B-1a population or perhaps in immature $B220^{hi}$ PBs.

Steady-state turnover, but not number, of B-1a cells is increased in *Nr4a1*$^{-/-}$ mice

To our surprise, despite expansion of B-1a–derived IgM PCs, precursor B-1a cell numbers and proportions did not differ significantly between WT and *Nr4a1*$^{-/-}$ mice (Fig. 5G, Supplemental Figs. 1D, 2G). We reasoned that if greater numbers of B-1a cells were exiting this compartment to divide and differentiate into IgM PCs in *Nr4a1*$^{-/-}$ mice, we would expect to see a compensatory increase in homeostatic renewal to maintain a normal B-1a compartment. To probe the rate of B-1a cell turnover, WT and *Nr4a1*$^{-/-}$ mice were fed BrdU in their drinking water for 2 wk, and incorporation into newly formed B-1a cells was assessed by intracellular staining (5). We find increased BrdU labeling in *Nr4a1*$^{-/-}$ B-1a cells but not in other compartments, suggesting a selective role for Nur77 in regulating the turnover of the B-1a compartment (Fig. 5H, Supplemental Fig. 2J).

Nur77 restrains T-independent immune responses by B-1a cells

In addition to generating natural IgM under steady-state conditions, B-1a cells mount IgM Ab responses to infection and immunization. To determine whether Nur77 deficiency also impacts these responses, WT and *Nr4a1*$^{-/-}$ mice were immunized i.p. with the T-independent immunogen NP-Ficoll. *Nr4a1*$^{-/-}$ mice produced enhanced and persistent NP-specific IgM titers, suggesting that Nur77 serves to restrain Ag-dependent B-1a humoral immune responses in the steady-state, as well as in response to acute antigenic stimulation (Fig. 5I). It remains to be established whether other innate-like B cell subsets, such as B-1b and MZ B-2 cells, may contribute to enhanced humoral immune responses in the absence of Nur77.

DISCUSSION

B-1a cells are actively selected for germline-encoded self-reactivity (3, 30). Using the Nur77-eGFP reporter, we show that Ag receptors of B-1a cells are chronically engaged by endogenous Ags under steady-state conditions in vivo (Figs. 1, 2). Constitutive expression of ITIM-containing inhibitory receptors is critical to maintain B-1a cells in a quiescent state in the face of chronic self-antigen stimulation. Disruption of ITIM function by deletion of Siglec-G, CD22, Shp-1, and CD5 in B-1a cells results in enhanced BCR signal transduction along with concomitant expansion of the B-1a compartment (5–8). More recently, the IgM Fc receptor was shown to restrain B-1 cell expansion and natural IgM production, possibly mediating a negative-feedback loop(31). In marked contrast to these genetic perturbations, Nur77-deficient B-1a cells do not exhibit enhanced proximal BCR signal transduction (Supplemental Fig. 2K), nor are B-1a cell numbers expanded in these mice (Fig. 5G). Rather, we find marked expansion of B-1a–derived immature and mature natural IgM PCs (Figs. 4, 5A–E), suggesting that Nur77 plays a unique role in restraining PC differentiation of B-1a cells. Moreover, the broad range of IgM concentration and IgM PC expansion observed in individual *Nr4a1*$^{-/-}$ mice, in contrast to tightly controlled and uniform levels in WT mice, imply a stochastic component to development of this phenotype (Figs. 3A, 4B, 4D, 5C, Supplemental Fig. 2B). We propose that this variation reflects the underlying biology of this system, in which intermittent encounter of B-1a cells with endogenous Ag under steady-state conditions (rather than an acute stimulus) drives PC expansion.

We provide several independent and complementary lines of evidence to argue that expanded serum IgM and IgM PCs in *Nr4a1*$^{-/-}$ mice originate from the B-1a compartment. Radiation chimeras into which WT or *Nr4a1*$^{-/-}$ allotype-marked PerC cells are adoptively transferred exhibit good reconstitution of B-1a cells but poor reconstitution of B-1b and B-2 cells, suggesting that B-1a cells are the most likely source of excess serum IgM in chimeric mice receiving *Nr4a1*$^{-/-}$ PerC cells (Fig. 3E, Supplemental Fig. 1J). Furthermore, the B-1b compartment harbors few PtC-specific B cells, whereas PtC^{+} cells make up 30–50% of the B-1a compartment (Supplemental Fig. 1C) (26). Because expanded IgM PCs in *Nr4a1*$^{-/-}$ mice include PtC-specific cells, these PCs likely originate in the B-1a compartment (Supplemental Fig. 2E). Moreover, excess serum IgM in *Nr4a1*$^{-/-}$ mice retains reactivity to the canonical B-1a specificity phosphorylcholine (Supplemental Fig. 1G, 1H). Finally, we present two pieces of strong circumstantial evidence to bolster these conclusions: B-1a cells, but not B-1b cells, express high levels of reporter Nur77-eGFP (Fig. 1F), and B-1a cells, but not B-1b cells, exhibit increased turnover in the absence of Nur77, as marked by BrdU incorporation (Fig. 5H, Supplemental Fig. 2J). These data collectively argue that Nur77 plays a cell-intrinsic role in B-1a cells to drive expansion of IgM PCs under steady-state conditions. However, because radiation chimeras were generated with transfer of PerC cells rather than purified B-1a cells, it remains possible that transferred *Nr4a1*$^{-/-}$ myeloid populations may contribute to these phenotypes. Conditional deletion of *Nr4a1* in B cells will be important to exclude this possibility.

Loss of Nur77 perturbs the normal repertoire of B-1a cells and natural IgM PCs. The frequency of PtC^{+} B-1a cells is reduced in *Nr4a1*$^{-/-}$ mice (Supplemental Fig. 2H, 2I). This may be due to impaired selection into this compartment, impaired self-renewal, or perhaps increased exit. These possibilities may be distinguished by tracking the B-1a repertoire at early time points in fetal development when the compartment is initially selected. Because PtC^{+} B-1a cells express higher levels of Nur77-eGFP (Fig. 2B, 2C), they may be more dependent than other specificities upon Nur77 expression to restrain their activation in response to chronic Ag stimulation; in the absence of Nur77, PtC^{+} B-1a cells may preferentially leave the compartment by differentiating into IgM PCs. Surprisingly, although absolute numbers of PtC^{+} IgM PCs are expanded in the absence of Nur77, their relative contribution to the total IgM PC compartment is reduced by half in *Nr4a1*$^{-/-}$ mice (Supplemental Fig. 2E, 2F). Deep sequencing of CDR3s from the B-1a and IgM PC compartments of WT and *Nr4a1*$^{-/-}$ mice will establish whether certain clones are preferentially recruited into the PC compartment or are selectively excluded.

Although ELISPOTs confirm that bona fide IgM ASCs are expanded in *Nr4a1*$^{-/-}$ mice, their frequency is not as high as that of IgM PCs identified by intracellular IgM staining (Fig. 4B–E, Supplemental Fig. 2B). In contrast, quantification of WT IgM PCs by flow staining and ELISPOT agree well (Figs. 4B–E, 5C, Supplemental Fig. 2B). About half of IgM PCs in Nr4a1$^{-/-}$ mice exhibit a B220^{hi} phenotype and retain elevated levels of Nur77-eGFP reporter expression, suggesting that they represent immature PCs or PBs (Fig. 5A–F). It is likely that these cells do not secrete high amounts of IgM and, therefore, may account for the discrepancy between ELISPOT and flow data. Indeed, quantification of B220^{lo} IgM PCsin*Nr4a1*$^{-/-}$ and WT mice correlates well with ELISPOT data (Figs. 4D, 5E). Although mature B220^{lo} IgM PCs are increased in *Nr4a1*$^{-/-}$ mice (Fig. 5E), B220^{hi} immature IgM

PCs/PBs are disproportionately expanded (~20-fold; Fig. 5D). It is possible that they are generated at higher numbers, expand more, and/or survive better in the absence of Nur77. Their accumulation relative to $B220^{lo}$ IgM PCs in *Nr4a1*$^{-/-}$ mice also implies that the terminally differentiated IgM PC compartment may be constrained by a limited survival niche. To our knowledge, this expansion of $B220^{hi}$ IgM PCs is a unique phenotype and, therefore, reveals a novel Nur77-dependent checkpoint in the generation of natural IgM PCs.

The PC program that Nur77 restrains is likely to be Irf4 and Blimp-1 dependent; expanded IgM PCs in *Nr4a1*$^{-/-}$ mice express high levels of Irf4 and resemble canonical Blimp-1–dependent natural IgM ASCs in their upregulation of CD138 (4). Indeed, it has been suggested that Irf4 can be directly repressed by Nur77 (32). Future work will be critical to further dissect the transcriptional mechanism by which Nur77 regulates PC differentiation of B-1a cells. Nur77 also mediates Ag-dependent cell death in T cells and may do so, at least in part, independently of transcription via direct interaction with Bcl-2 family members (11, 12, 33). An analogous mechanism may restrain B-1a cells from generating an expanded PC compartment.

We demonstrate that steady-state IgM PC generation increased in the absence of Nur77, as well as that Ag-specific IgM is increased in response to immunization with the model TI-2 Ag NP-Ficoll. Thus, our observations have important implications for understanding immune homeostasis, as well as for vaccine development. Although Nr4a family members have no known endogenous ligands, naturally occurring and synthetically derived agonists and antagonists have been described (34, 35). To our knowledge, we provide the first proof-of-principle data to suggest that a Nur77-specific antagonist could function as a “universal adjuvant” for T-independent vaccines, such as the widely used pneumococcal polysaccharide vaccine PPSV23. Additional studies of Ig isotypes, specificities, and kinetics of response to immunization will be critical to further explore this potential application.

Supplementary Material

Refer to Web version on PubMed Central for supplementary material.

Acknowledgments

We thank Al Roque for help with animal husbandry.

This work was supported by the Howard Hughes Medical Institute Medical Research Fellows program (to J.H.), National Institute of Allergy and Infectious Diseases Grant 5T32AI007334-28 (to C.T.), National Science Foundation Graduate Research Fellowship 1650113 (to M.N.), and the Rheumatology Research Foundation (to J.Z.).

Abbreviations

ASC	Ab-secreting cell
BM	bone marrow
HEL	hen egg lysozyme
IgHEL	hen egg lysozyme–specific BCR

PB	plasmablast
PC	plasma cell
PerC	peritoneal cavity
PtC	phosphatidylcholine
SA	streptavidin
Tg	transgenic
WT	wild-type

References

1. Baumgarth N. B-1 cell heterogeneity and the regulation of natural and antigen-induced IgM production. Front Immunol. 2016; 7:324. [PubMed: 27667991]
2. Yang Y, Wang C, Yang Q, Kantor AB, Chu H, Ghosn EE, Qin G, Mazmanian SK, Han J, Herzenberg LA. Distinct mechanisms define murine B cell lineage immunoglobulin heavy chain (IgH) repertoires. eLife. 2015; 4:e09083. [PubMed: 26422511]
3. Bendelac A, Bonneville M, Kearney JF. Autoreactivity by design: innate B and T lymphocytes. Nat Rev Immunol. 2001; 1:177–186. [PubMed: 11905826]
4. Savage HP, Yenson VM, Sawhney SS, Mousseau BJ, Lund FE, Baumgarth N. Blimp-1–dependent and -independent natural antibody production by B-1 and B-1–derived plasma cells. J Exp Med. 2017; 214:2777–2794. [PubMed: 28698287]
5. Hoffmann A, Kerr S, Jellusova J, Zhang J, Weisel F, Wellmann U, Winkler TH, Kneitz B, Crocker PR, Nitschke L. Siglec-G is a B1 cell–inhibitory receptor that controls expansion and calcium signaling of the B1 cell population. Nat Immunol. 2007; 8:695–704. [PubMed: 17572677]
6. Jellusova J, Wellmann U, Amann K, Winkler TH, Nitschke L. CD22 × Siglec-G double-deficient mice have massively increased B1 cell numbers and develop systemic autoimmunity. J Immunol. 2010; 184:3618–3627. [PubMed: 20200274]
7. Pao LI, Lam KP, Henderson JM, Kutok JL, Alimzhanov M, Nitschke L, Thomas ML, Neel BG, Rajewsky K. B cell–specific deletion of protein-tyrosine phosphatase Shp1 promotes B-1a cell development and causes systemic autoimmunity. Immunity. 2007; 27:35–48. [PubMed: 17600736]
8. Bikah G, Carey J, Ciallella JR, Tarakhovsky A, Bondada S. CD5-mediated negative regulation of antigen receptor-induced growth signals in B-1 B cells. Science. 1996; 274:1906–1909. [PubMed: 8943203]
9. Maxwell MA, Muscat GE. The NR4A subgroup: immediate early response genes with pleiotropic physiological roles. Nucl Recept Signal. 2006; 4:e002. [PubMed: 16604165]
10. Calnan BJ, Szychowski S, Chan FK, Cado D, Winoto A. A role for the orphan steroid receptor Nur77 in apoptosis accompanying antigen-induced negative selection. Immunity. 1995; 3:273–282. [PubMed: 7552993]
11. Woronicz JD, Calnan B, Ngo V, Winoto A. Requirement for the orphan steroid receptor Nur77 in apoptosis of T-cell hybridomas. Nature. 1994; 367:277–281. [PubMed: 8121493]
12. Liu ZG, Smith SW, McLaughlin KA, Schwartz LM, Osborne BA. Apoptotic signals delivered through the T-cell receptor of a T-cell hybrid require the immediate-early gene nur77. Nature. 1994; 367:281–284. [PubMed: 8121494]
13. Lee SL, Wesselschmidt RL, Linette GP, Kanagawa O, Russell JH, Milbrandt J. Unimpaired thymic and peripheral T cell death in mice lacking the nuclear receptor NGFI-B (Nur77). Science. 1995; 269:532–535. [PubMed: 7624775]
14. Mullican SE, Zhang S, Konopleva M, Ruvolo V, Andreeff M, Milbrandt J, Conneely OM. Abrogation of nuclear receptors Nr4a3 and Nr4a1 leads to development of acute myeloid leukemia. Nat Med. 2007; 13:730–735. [PubMed: 17515897]

15. Boudreaux SP, Ramirez-Herrick AM, Duren RP, Conneely OM. Genome-wide profiling reveals transcriptional repression of MYC as a core component of NR4A tumor suppression in acute myeloid leukemia. Oncogenesis. 2012; 1:e19. [PubMed: 23552735]
16. Sekiya T, Kashiwagi I, Yoshida R, Fukaya T, Morita R, Kimura A, Ichinose H, Metzger D, Chambon P, Yoshimura A. Nr4a receptors are essential for thymic regulatory T cell development and immune homeostasis. Nat Immunol. 2013; 14:230–237. [PubMed: 23334790]
17. Sekiya T, Nakatsukasa H, Lu Q, Yoshimura A. Roles of transcription factors and epigenetic modifications in differentiation and maintenance of regulatory T cells. Microbes Infect. 2016; 18:378–386. [PubMed: 26970203]
18. Hanna RN, Carlin LM, Hubbeling HG, Nackiewicz D, Green AM, Punt JA, Geissmann F, Hedrick CC. The transcription factor NR4A1 (Nur77) controls bone marrow differentiation and the survival of Ly6C^{-} monocytes. Nat Immunol. 2011; 12:778–785. [PubMed: 21725321]
19. Thomas GD, Hanna RN, Vasudevan NT, Hamers AA, Romanoski CE, McArdle S, Ross KD, Blatchley A, Yoakum D, Hamilton BA, et al. Deleting an Nr4a1 super-enhancer sub-domain ablates Ly6C(low) monocytes while preserving macrophage gene function. Immunity. 2016; 45:975–987. [PubMed: 27814941]
20. Carlin LM, Stamatiades EG, Auffray C, Hanna RN, Glover L, Vizcay-Barrena G, Hedrick CC, Cook HT, Diebold S, Geissmann F. Nr4a1-dependent Ly6C(low) monocytes monitor endothelial cells and orchestrate their disposal. Cell. 2013; 153:362–375. [PubMed: 23582326]
21. Hanna RN, Shaked I, Hubbeling HG, Punt JA, Wu R, Herrley E, Zaugg C, Pei H, Geissmann F, Ley K, Hedrick CC. NR4A1 (Nur77) deletion polarizes macrophages toward an inflammatory phenotype and increases atherosclerosis. Circ Res. 2012; 110:416–427. [PubMed: 22194622]
22. Mueller J, Matloubian M, Zikherman J. Cutting edge: an in vivo reporter reveals active B cell receptor signaling in the germinal center. J Immunol. 2015; 194:2993–2997. [PubMed: 25725108]
23. Zikherman J, Parameswaran R, Weiss A. Endogenous antigen tunes the responsiveness of naive B cells but not T cells. Nature. 2012; 489:160–164. [PubMed: 22902503]
24. Goodnow CC, Crosbie J, Adelstein S, Lavoie TB, Smith-Gill SJ, Brink RA, Pritchard-Briscoe H, Wotherspoon JS, Loblay RH, Raphael K, et al. Altered immunoglobulin expression and functional silencing of self-reactive B lymphocytes in transgenic mice. Nature. 1988; 334:676–682. [PubMed: 3261841]
25. Skrzypczynska KM, Zhu JW, Weiss A. Positive regulation of Lyn kinase by CD148 is required for B cell receptor signaling in B1 but not B2 B cells. Immunity. 2016; 45:1232–1244. [PubMed: 27889108]
26. Mercolino TJ, Locke AL, Afshari A, Sasser D, Travis WW, Arnold LW, Haughton G. Restricted immunoglobulin variable region gene usage by normal Ly-1 (CD5+) B cells that recognize phosphatidyl choline. J Exp Med. 1989; 169:1869–1877. [PubMed: 2499651]
27. Reynolds AE, Kuraoka M, Kelsoe G. Natural IgM is produced by CD5^{-} plasma cells that occupy a distinct survival niche in bone marrow. J Immunol. 2015; 194:231–242. [PubMed: 25429072]
28. Chang X, Li B, Rao A. RNA-binding protein hnRNPLL regulates mRNA splicing and stability during B-cell to plasma-cell differentiation. Proc Natl Acad Sci USA. 2015; 112:E1888–E1897. [PubMed: 25825742]
29. Blanc P, Moro-Sibilot L, Barthly L, Jagot F, This S, Bernard S de, Buffat L, Dussurgey S, Colisson R, Hobeika E, et al. Mature IgM-expressing plasma cells sense antigen and develop competence for cytokine production upon antigenic challenge. Nat Commun. 2016; 7:13600. [PubMed: 27924814]
30. Hayakawa K, Asano M, Shinton SA, Gui M, Wen LJ, Dashoff J, Hardy RR. Positive selection of anti–Thy-1 autoreactive B-1 cells and natural serum autoantibody production independent from bone marrow B cell development. J Exp Med. 2003; 197:87–99. [PubMed: 12515816]
31. Nguyen TT, Kläsener K, Zürn C, Castillo PA, Brust-Mascher I, Imai DM, Bevins CL, Reardon C, Reth M, Baumgarth N. The IgM receptor FcμR limits tonic BCR signaling by regulating expression of the IgM BCR. Nat Immunol. 2017; 18:321–333. [PubMed: 28135254]
32. Nowyhed HN, Huynh TR, Thomas GD, Blatchley A, Hedrick CC. Cutting edge: the orphan nuclear receptor Nr4a1 regulates CD8+ T cell expansion and effector function through direct repression of Irf4. J Immunol. 2015; 195:3515–3519. [PubMed: 26363057]

33. Lin B, Kolluri SK, Lin F, Liu W, Han YH, Cao X, Dawson MI, Reed JC, Zhang XK. Conversion of Bcl-2 from protector to killer by interaction with nuclear orphan receptor Nur77/TR3. Cell. 2004; 116:527–540. [PubMed: 14980220]

34. Zhan YY, Chen Y, Zhang Q, Zhuang JJ, Tian M, Chen HZ, Zhang LR, Zhang HK, He JP, Wang WJ, et al. The orphan nuclear receptor Nur77 regulates LKB1 localization and activates AMPK. Nat Chem Biol. 2012; 8:897–904. [PubMed: 22983157]

35. Zhan Y, Du X, Chen H, Liu J, Zhao B, Huang D, Li G, Xu Q, Zhang M, Weimer BC, et al. Cytosporone B is an agonist for nuclear orphan receptor Nur77. Nat Chem Biol. 2008; 4:548–556. [PubMed: 18690216]

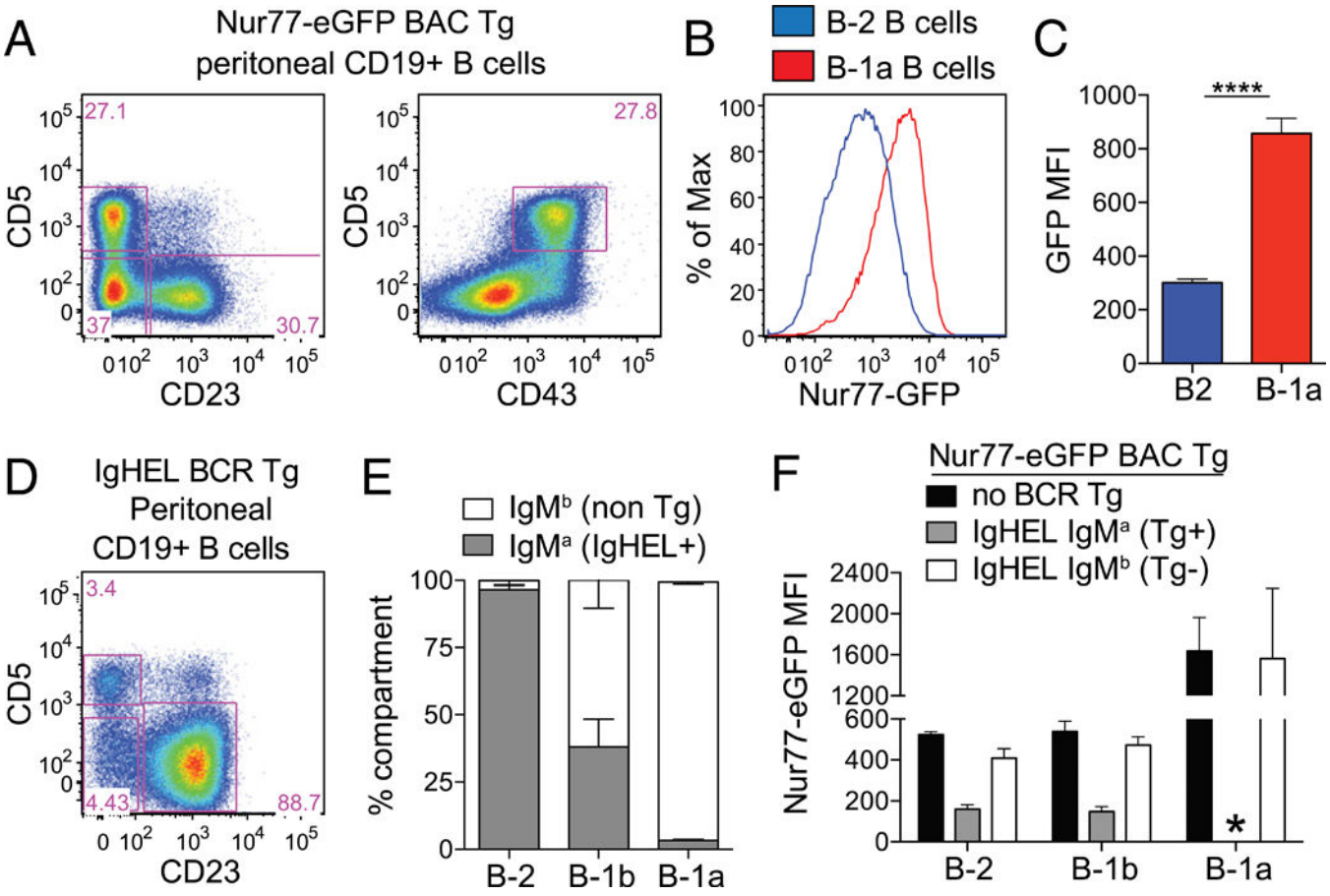

FIGURE 1. Nur77-eGFP reporter expression is upregulated in B1-a B cells in an Ag-dependent manner

(**A**) PerC cells were stained to detect B cell subsets. Representative plots of $CD19^+$ cells show gating to identify B-1a ($CD5^+$ $CD23^-$ $CD43^+$), B-1b ($CD23^-$ $CD5^-$), and B-2 ($CD23^+$ $CD5^-$) cells. (**B**) PerC cells from Nur77-eGFP reporter mice were stained and gated as in (A). Representative graph depicts GFP fluorescence in B-1a and B-2 cells. (**C**) Bar graph depicts GFP mean fluorescence intensity (MFI) (± SEM) from cells, as gated in (A) and (B), in $n = 5$ biological replicates. $^{****}p < 0.0001$, unpaired t test. (**D**) PerC cells from IgHEL Tg Nur77-eGFP reporter mice were stained and gated as in (A) to identify B-1a, B-1b, and B-2 cells. (**E**) B cell subsets, gated as in (D), were further subdivided on the basis of IgM^a expression to identify BCR-Tg^+ cells (gated as in Supplemental Fig. 1A). Bar graph depicts the percentage (± SEM) of IgM^a cells within each B cell subset in $n = 3$ biological replicates. (**F**) Nur77-eGFP mice, with or without IgHEL Tg, were stained and gated as in (D) and (E) to identify Tg^+ and Tg^- cells from each PerC B cell compartment. Bar graph depicts GFP MFI (± SEM) in $n = 3$ biological replicates. *No data because there are no IgM^a B-1a cells detected in IgHEL Tg mice, as shown in (E).

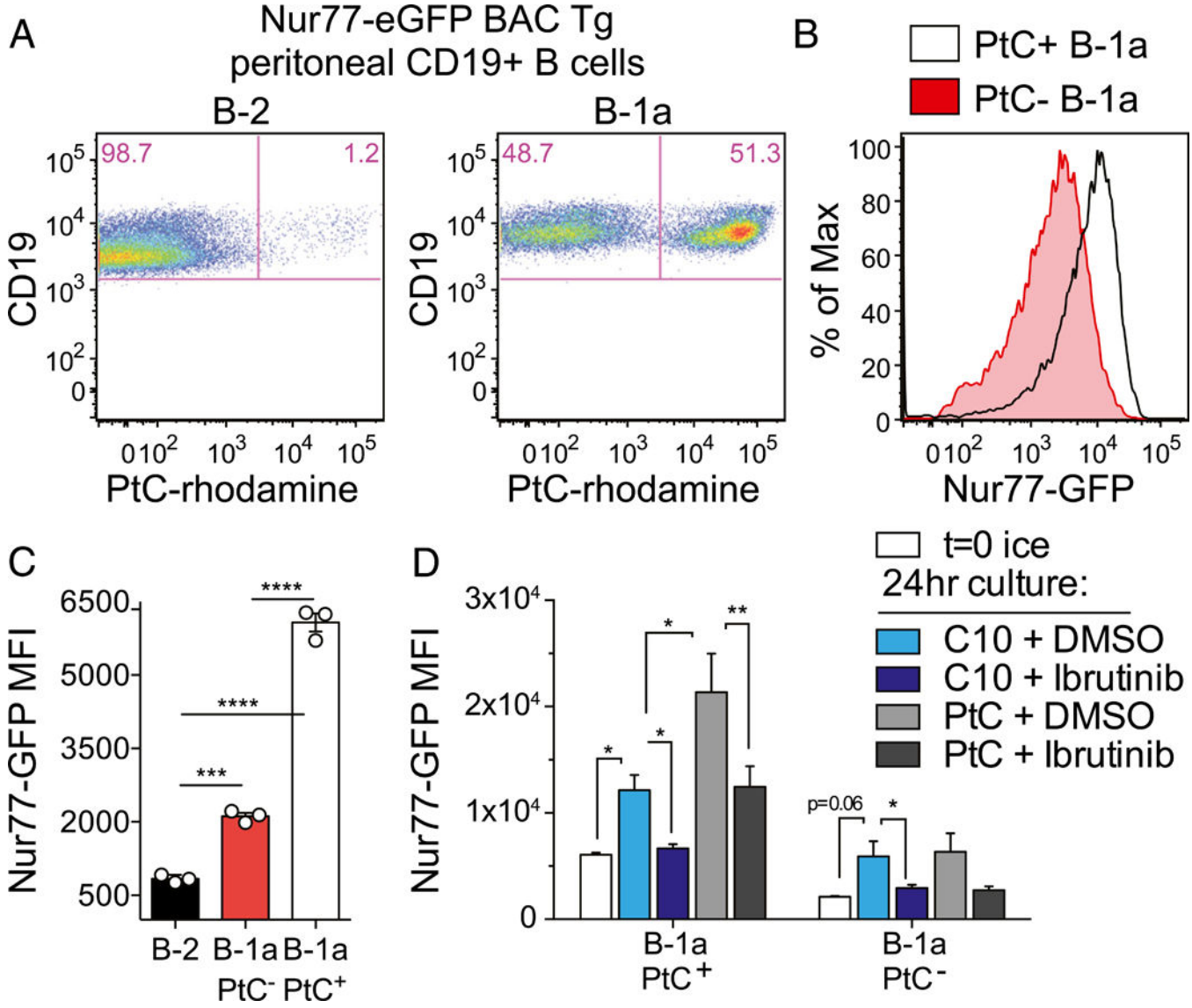

FIGURE 2. Nur77-eGFP expression identifies self-reactive PtC-specific B-1a cells in vivo

(**A**) PerC cells from Nur77-eGFP reporter mice were stained immediately ex vivo with surface markers and PtC-rhodamine liposomes to identify B cell subsets (as gated in Fig. 1A). Representative plots show PtC^+ B cells in the B-2 and B-1a compartments of these mice. (**B**) Line graph depicts Nur77-eGFP expression in PtC^+ and PtC^- B-1a cells gated as in (A). (**C**) Graph depicts Nur77-eGFP mean fluorescence intensity (MFI) (± SEM) in PerC B cell subsets stained and collected by flow immediately ex vivo and gated as in (A). $^{***}p < 0.0005$, $^{****}p < 0.0001$, unpaired *t* test. (**D**) PerC cells from Nur77-eGFP reporter mice were incubated in complete culture media for 24 h with ibrutinib or DMSO in the presence or absence of PtC-rhodamine liposomes. Cells were then stained, collected, and analyzed as in (A). Bar graph depicts GFP MFI (± SEM) in PtC^+ and PtC^- B-1a cells in $n = 3$ biological replicates. $^{*}p < 0.05$, $^{**}p < 0.005$, ratio paired *t* test.

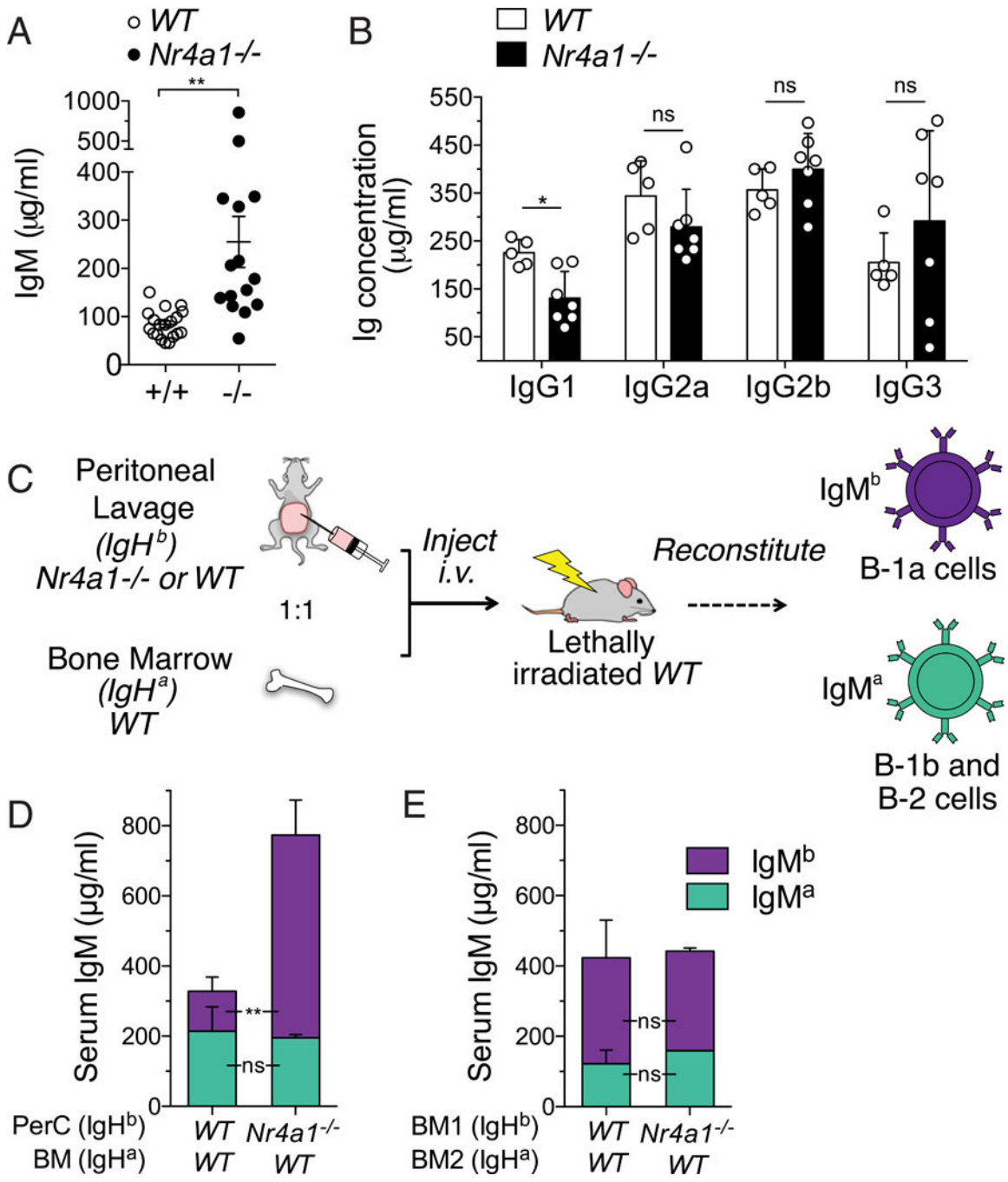

FIGURE 3. Excess natural serum IgM in *Nr4a1*$^{-/-}$ mice arises from the B-1a compartment

(**A**) Sera from WT and *Nr4a1*$^{-/-}$ mice were collected at age 10–15 wk. Graph shows IgM concentration quantified by ELISA (± SEM). $^{**}p < 0.005$, unpaired *t* test with Welch's correction. (**B**) Sera from WT and *Nr4a1*$^{-/-}$ mice were collected at 16 wk of age. Bar graph shows IgG isotype concentration quantified by ELISA (± SEM). (**C**) Schematic diagram of strategy to generate radiation chimeras harboring selective B-1a reconstitution with allotype-marked *Nr4a1*$^{-/-}$ cells. (**D**) Serum from chimeric mice, generated as in (C), was collected 7 wk after irradiation. Bar graph depicts concentration (± SEM) of IgM^a and IgM^b allotypes in

$n = 4$ biological replicates. (**E**) Serum from chimeric mice generated with a 1:1 mixture of IgH^a WT BM mixed with WT or *Nr4a1*$^{-/-}$ IgH^b BM was collected 6 wk after irradiation. Bar graph depicts the concentration of IgM^a and IgM^b allotypes (± SEM) in $n = 3$ or 4 biological replicates. $^{*}p < 0.05$, $^{**}p < 0.005$, unpaired *t* test (B–E). ns, not significant.

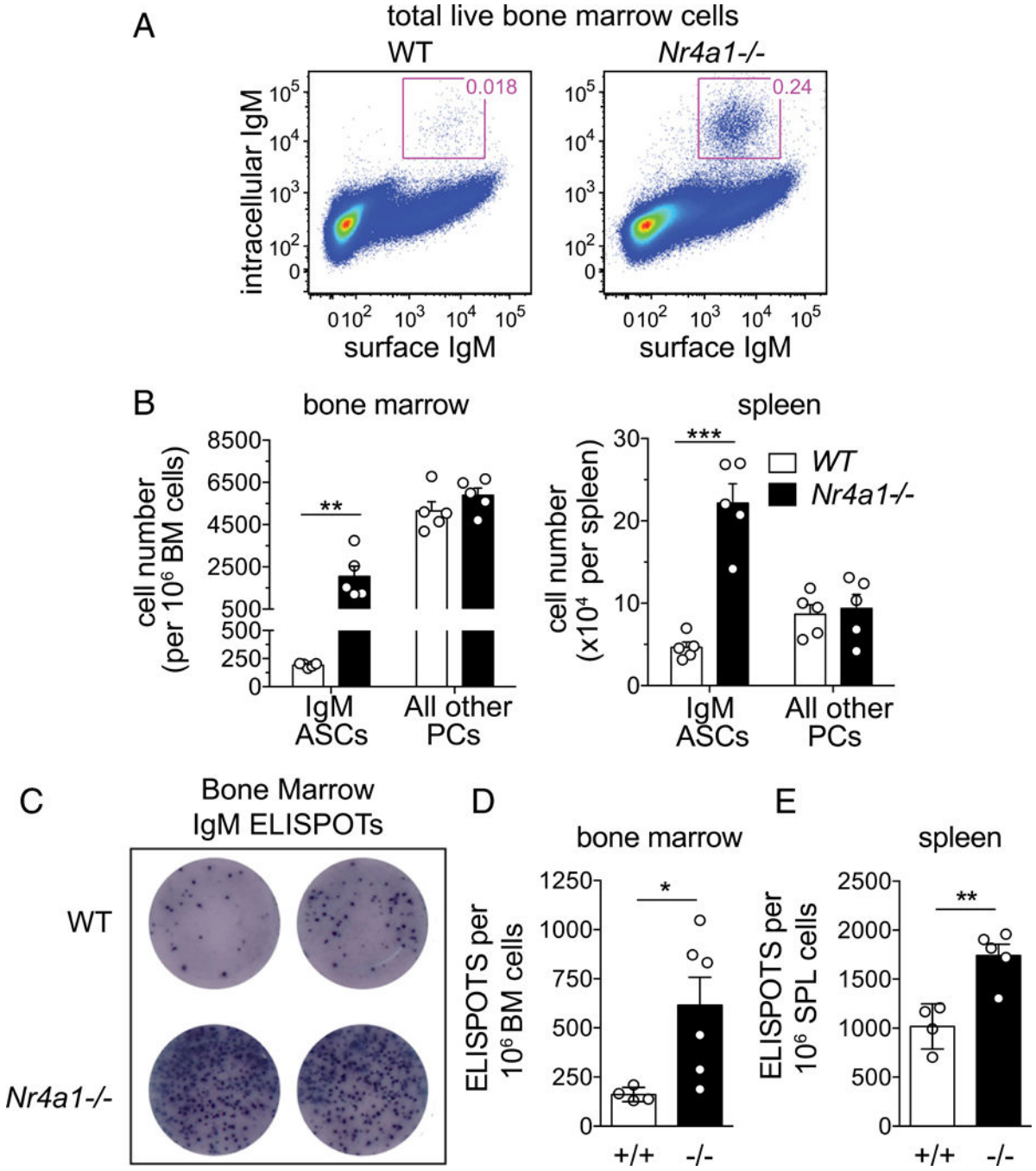

FIGURE 4. IgM ASCs are expanded in *Nr4a1*$^{-/-}$ mice

(**A**) WT and *Nr4a1*$^{-/-}$ BM cells were stained for surface and intracellular IgM. Representative plots show gating to identify putative IgM ASCs. (**B**) Bar graphs depict number of IgM ASCs from BM and spleen, gated as in (A), as well as isotype-switched PCs identified on the basis of high expression of CD138 and IgM^{-}. Data are mean ± SEM. $^{**}p < 0.005$, $^{***}p < 0.0005$, unpaired *t* test. (**C**) Representative IgM ASC ELISPOTs from WT and *Nr4a1*$^{-/-}$ BM (5×10^5 cells per well). (**D**) Bar graph shows quantification of mean (± SEM) IgM ELISPOT number in BM, as depicted in (C). $^{*}p < 0.05$, unpaired *t* test with Welch's

correction. (**E**) Bar graph shows quantification of mean (± SEM) IgM ELISPOT number in spleen. $^{**}p < 0.005$, unpaired *t* test.

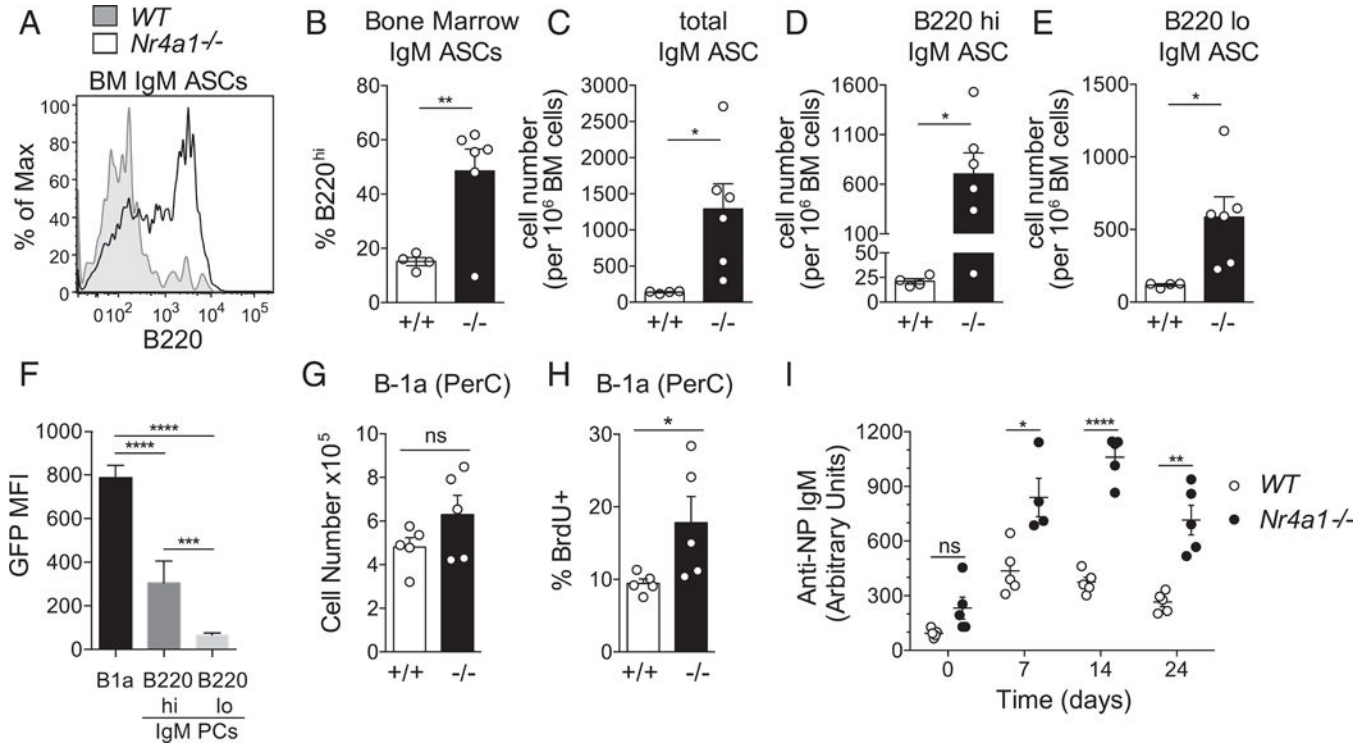

FIGURE 5. B-1a cells turnover more quickly and accumulate as immature IgM ASCs in the absence of Nur77

(**A**) Representative line graph depicts B220 surface expression on BM IgM ASCs from WT and knockout (KO) mice, as gated in Fig. 4A. (**B**) Bar graph depicts mean percentage (± SEM) of $B220^{hi}$ IgM ASCs, as gated in (A). (**C**) Bar graph shows quantification of total BM IgM ASCs detected by intracellular staining for IgM and gated as in Fig. 4A. Mice analyzed correspond to those used in the ELISPOT assay (Fig. 4C, 4D). (**D**) Bar graph depicts mean (± SEM) cell number of $B220^{hi}$ IgM ASCs from (C). (**E**) Bar graph depicts mean (± SEM) cell number of $B220^{lo}$ IgM ASCs from (C). (**F**) PerC cells and BM from Nur77-eGFP reporter mice were stained to detect B-1a cells (see Fig. 1A gates), as well as $B220^{hi}$ and $B220^{lo}$ IgM ASCs [see gates in Fig. 4A and (A)]. Bar graph depicts GFP MFI (± SEM) in $n = 4$ WT and $n = 6$ KO biological replicates. (**G**) Bar graph depicts mean (± SEM) B-1a cell number in PerC cells from WT and KO mice. (**H**) WT and KO mice were given BrdU in water for 2 wk. Upon harvest, PerC cells (quantified in E) were surface stained and permeabilized to detect BrdU incorporation. Bar graph depicts the mean (± SEM) percentage of $BrdU^+$ B-1a cells. (**I**) WT and KO mice were immunized i.p. with NP-Ficoll, and sera were collected at baseline and weekly for 3 wk. Graph depicts relative concentration (± SEM) of NP-specific IgM in sera, as quantified by ELISA. $^{*}p < 0.05$, $^{**}p < 0.005$, $^{***}p < 0.0005$, $^{****}p < 0.0001$, unpaired *t* test (B, D–G, I, and J), unpaired *t* test with Welch's correction (C). ns, not significant.